

Nuclear-Level Effective Theory of $\mu \rightarrow e$ Conversion

Evan Rule,¹ W. C. Haxton,^{1,2} and Kenneth McElvain¹

¹*Department of Physics, University of California, Berkeley, CA 94720, USA*

²*Lawrence Berkeley National Laboratory, Berkeley, CA 94720, USA*

(Dated: September 16, 2022)

The Mu2e and COMET $\mu \rightarrow e$ conversion experiments are expected to significantly advance limits on new sources of charged lepton flavor violation (CLFV). Almost all theoretical work in the field has focused on just two operators. However, general symmetry arguments lead to a $\mu \rightarrow e$ conversion rate with six response functions, each of which, in principle, is observable by varying nuclear properties of targets. We construct a nucleon-level nonrelativistic effective theory (NRET) to clarify the microscopic origin of these response functions and to relate rate measurements in different targets. This exercise identifies three operators and their small parameters that control the NRET operator expansion. We note inconsistencies in past treatments of these parameters. The NRET is technically challenging, involving 16 operators, several distorted electron partial waves, bound muon upper and lower components, and an exclusive nuclear matrix element. We introduce a trick for treating the electron Coulomb effects accurately, which enables us to include all of these effects while producing transition densities whose one-body matrix elements can be evaluated analytically, greatly simplifying the nuclear physics. We derive bounds on operator coefficients from existing and anticipated $\mu \rightarrow e$ conversion experiments. We discuss how similar NRET formulations have impacted dark matter phenomenology, noting that the tools this community has developed could be adapted for CLFV studies.

$\mu \rightarrow e$ conversion and other charged lepton flavor violation (CLFV) processes have long been recognized as sensitive tests of new physics beyond the standard model [1–4]. The Mu2e [5, 6] experiment at Fermilab and the COMET [7, 8] experiment at J-PARC aim to improve existing limits on the ratio of rates

$$R_{\mu e} = \frac{\omega[\mu^- + (A, Z) \rightarrow e^- + (A, Z)]}{\omega[\mu^- + (A, Z) \rightarrow \nu_\mu + (A, Z - 1)]} \quad (1)$$

by four orders of magnitude, probing new physics to scales of $\sim 10^4$ TeV. Both experiments will use the relatively light target ^{27}Al and focus on captures that leave the nucleus in its ground state. The elastic process maximizes the energy of the outgoing electron, $E_e \sim m_\mu - E_\mu^{\text{bind}}$ neglecting nuclear recoil, where E_μ^{bind} is the (positive) muon binding energy. This minimizes the standard-model background from the three-body decay $\mu^- \rightarrow e^- + \nu_\mu + \bar{\nu}_e$, as few electrons are produced near the endpoint.

Consequently, the CLFV operators contributing to $\mu \rightarrow e$ conversion are constrained by the nearly exact parity and CP of the nuclear ground state: these symmetries eliminate some CLFV operators entirely and restrict the contributing multipoles of those that do survive. Our aim is to determine the constraints that can be imposed on the coefficients of the operators of a general nucleon-level effective theory (ET) of CLFV, thereby identifying what can and cannot be learned from elastic $\mu \rightarrow e$ conversion.

The form of the $\mu \rightarrow e$ rate can be deduced from general considerations, including Galilean/ro-

tational invariance, the good parity (P) and CP of the nuclear ground state, and the symmetry transformation properties of the available charges and currents, and their gradients and curls. The detailed derivation is included in an accompanying technical paper [9]. The resulting rate consists of six response functions (and two interference terms), each of which is, in principle, observable by making measurements in multiple nuclear targets selected for their ground-state properties, allowing one to emphasize or suppress certain interactions.

Rates in different nuclei can be related using a nucleon-level interaction, the general form of which is determined by nonrelativistic effective theory (NRET). One constructs a general CLFV interaction from the available operators — including, in this case, the charge and spin operators for the leptons and nucleons, the nucleon relative velocity operator \vec{v}_N (conjugate to the internucleon coordinate \vec{r}), and the muon velocity operator \vec{v}_μ (conjugate to the coordinate describing the bound muon relative to the nuclear center-of-mass). The construction follows that performed for dark matter (DM) phenomenology [10–12]. When this interaction is embedded in the nucleus, an additional operator enters due to nuclear compositeness, $\vec{q} \cdot \vec{r} \sim 1$. As in DM direct detection, the three-momentum transfer q is comparable to the nuclear size, implying significant angular momentum transfer. Thus the nuclear physics is complex, requiring a multipole expansion.

NRET predictions of low-energy observables will be equivalent to those of higher-energy EFTs (if both

theories are expanded to the same order), but as fewer degrees of freedom are relevant at low energies, the NRET operator basis will be leaner and more efficient. The information extracted from experiment can then be ported upward, constraining higher level theories. A conceptual depiction of the process is captured in Fig. 4 of a DM Snowmass report [12], where considerable work has been invested in matching theories, most of which can be readily adapted to $\mu \rightarrow e$ conversion.

In NRET, one identifies a theory's small parameters and organizes the operator expansion accordingly. We find, associated with $\vec{q} \cdot \vec{r}$, \vec{v}_N , and \vec{v}_μ , the expansion parameters

$$y = \left(\frac{qb}{2}\right)^2 = 0.24 > \left|\left\langle\frac{\vec{v}_N}{2}\right\rangle\right| = 0.11 > \left|\left\langle\frac{\vec{v}_\mu}{2}\right\rangle\right| = 0.026$$

where the numerical values are those of Al. Here b is the oscillator parameter representing the nuclear size. The hierarchy of operators and the expansion parameters they generate should guide all treatments of $\mu \rightarrow e$ conversion, but this typically has not been the case. Table 1 of [9] provides a summary of the literature. Rate calculations have been done repeatedly for just two nuclear operators, $1_L 1_N$ and $\vec{\sigma}_L \cdot \vec{\sigma}_N$. The velocity operator \vec{v}_μ , which generates the muon's lower component, has been explored frequently but always with a restriction on the included electron partial waves of $|\kappa| = 1$, where κ is the Dirac quantum number, thereby limiting the expansion in y so that only the leading nuclear multipole is retained. This is done because otherwise the algebra is complicated, but the restriction — parametrically and numerically — typically generates an error larger than the \vec{v}_μ correction being made [9]. Here, we describe a formalism that treats \vec{v}_μ accurately and elegantly, including all multipoles. We find that \vec{v}_μ is a relatively uninteresting operator, playing no symmetry role and contributing only a 5% numerical correction to Al nuclear form factors.

In contrast, none of papers in Table 1 of [9] treats \vec{v}_N . This operator, parametrically larger than \vec{v}_μ , represents the $A - 1$ internal (Jacobi) internucleon velocities in the bound state. (The A th Jacobi velocity is \vec{v}_μ .) Without the inclusion of \vec{v}_N , the NRET rate is not consistent with the general form derived from symmetry arguments: Potentially important physics has been omitted. Further, this operator produces a novel form of coherence that operates only in certain nuclei like Al and Cu, where the Fermi sea fills only one of two spin-orbit subshells, $(\ell s)j = \ell \pm \frac{1}{2}$. While one would expect \vec{v}_N -dependent operators to be subleading, of $o\left(\frac{q}{m_N}\right) \sim \frac{1}{10}$, this co-

herence can elevate certain velocity-dependent operators to $o(1)$, where they can dominate rates even if operators like 1_N and $\vec{\sigma}_N$ are also present.

Leptonic Interactions: $\mu \rightarrow e$ conversion proceeds through the capture of a 1s muon bound by the nuclear Coulomb field and the emission of a highly relativistic electron. It is desirable, especially in heavier targets, to obtain the lepton wave functions from the Dirac equation, using an extended nuclear charge distribution [14–18]. The transition density then depends on a convolution of a nuclear density (which depends on the operator being studied), the muon wave functions, and various electron distorted waves that, in the absence of the Coulomb interaction, would correspond to the spherical wave expansion of $e^{i\vec{q} \cdot \vec{r}}$.

The muon quickly cascades to the 1s orbital as it comes to rest in a target. The Dirac solution is related to the muon's velocity operator through the approximate relationship [9]

$$\psi_{\kappa=-1} = \begin{bmatrix} ig(r)\xi_s \\ f(r)\vec{\sigma} \cdot \hat{r}\xi_s \end{bmatrix} \frac{1}{\sqrt{4\pi}} \sim \begin{bmatrix} \xi_s \\ \frac{\vec{\sigma} \cdot \vec{v}_\mu}{2}\xi_s \end{bmatrix} \frac{ig(r)}{\sqrt{4\pi}} \quad (2)$$

where ξ_s is the Pauli spinor. The normalization is

$$\int_0^\infty dr r^2 (g_\kappa^2(r) + f_\kappa^2(r)) = 1.$$

A linear expansion in \vec{v}_μ means retaining $f(r)$.

The electron produced in $\mu \rightarrow e$ conversion is ultra-relativistic. Deviations from a Dirac plane wave arise from the nuclear Coulomb attraction, which modestly enhances the wave function amplitude near the nucleus and shortens the wavelength. We account for these effects by a procedure familiar from electron scattering studies [21–23], replacement of \vec{q} in the Dirac plane wave by a shifted momentum \vec{q}_{eff} , yielding

$$U(q, s) e^{i\vec{q} \cdot \vec{x}} \rightarrow \sqrt{\frac{E_e}{2m_e}} \begin{pmatrix} \xi_x \\ \vec{\sigma} \cdot \hat{q}\xi_s \end{pmatrix} \frac{q_{\text{eff}}}{q} e^{i\vec{q}_{\text{eff}} \cdot \vec{x}}. \quad (3)$$

The local momentum q_{eff} is obtained from a constant potential whose depth is equated to the average of the Coulomb potential over the nuclear charge distribution. We find $q_{\text{eff}} = 110.81$ MeV and 112.43 MeV for ^{27}Al and ^{48}Ti , respectively. The effective momentum approximation, the Dirac plane-wave solution, and the Dirac Coulomb solution for ^{27}Al and ^{48}Ti are shown in Fig. 1. The q_{eff} approximation nicely accounts for the distortion. The results shown correspond to the $\kappa = -1$ state, but this approximation works equally well for other Dirac partial waves and remains accurate for high- Z targets of interest, such as W [9].

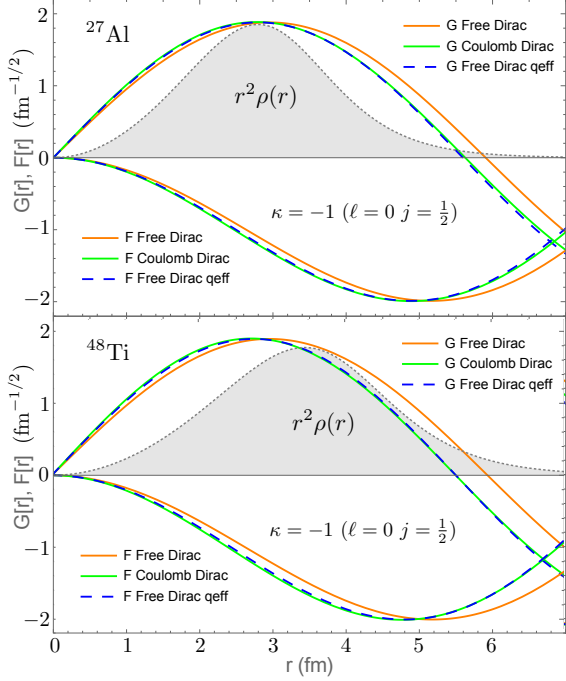


FIG. 1. Free and Coulomb Dirac solutions $G(r) = rg(r)$ and $F(r) = rf(r)$ are compared to the q_{eff} -shifted free Dirac solution for the relativistic electron. The nuclear charge distribution (shaded) used in the Coulomb calculation is also shown (arbitrary normalization).

The NRET construction: Eqs. (2) and (3) allow one to construct a nucleon-level NRET for $\mu \rightarrow e$ conversion that operates between Pauli spinors. Available operators include the lepton and nucleon identities 1_L and 1_N and five dimensionless Hermitian three-vectors

$$i\hat{q} = \frac{i\vec{q}}{|\vec{q}|}, \quad \vec{\sigma}_L, \quad \vec{\sigma}_N, \quad \vec{v}_N, \quad \vec{v}_\mu \quad (4)$$

The nuclear velocity operator has the symmetrized form $\vec{v}_N = (\vec{p}_i + \vec{p}_f)/(2m_N)$.

Omission of the velocity operators will produce a rate appropriate for a point nucleus, but not generate all projections of the vector current allowed by symmetry [9]. The addition of \vec{v}_N completes the NRET, and interesting new physics arises when \vec{v}_N -dependent operators are embedded in the nucleus. In contrast, \vec{v}_μ 's only role is to generate nuclear form factor corrections suppressed by the ratio of average values of the muon's lower and upper components $\langle f \rangle / \langle g \rangle$. We will omit this operator presently.

The NRET includes \vec{v}_N only linearly, as certain ambiguities arise in bound-state applications beyond first order [24]. The nucleon operators can be combined as $\vec{v}_N \cdot \vec{\sigma}_N$ and $\vec{v}_N \times \vec{\sigma}_N$, but not as the rank-

two tensor $[\vec{v}_N \otimes \vec{\sigma}_N]_2$, which would not triangulate between spin- $\frac{1}{2}$ nucleon states. As the interaction occurs at a fixed $q \sim m_\mu$, any propagator effects can be absorbed into the operator coefficients.

We identify a total of 16 independent operators

$$\begin{aligned} \mathcal{O}_1 &= 1_L 1_N & \mathcal{O}_9 &= \vec{\sigma}_L \cdot (i\hat{q} \times \vec{\sigma}_N) \\ \mathcal{O}'_2 &= 1_L i\hat{q} \cdot \vec{v}_N & \mathcal{O}_{10} &= 1_L i\hat{q} \cdot \vec{\sigma}_N \\ \mathcal{O}_3 &= 1_L i\hat{q} \cdot [\vec{v}_N \times \vec{\sigma}_N] & \mathcal{O}_{11} &= i\hat{q} \cdot \vec{\sigma}_L 1_N \\ \mathcal{O}_4 &= \vec{\sigma}_L \cdot \vec{\sigma}_N & \mathcal{O}_{12} &= \vec{\sigma}_L \cdot [\vec{v}_N \times \vec{\sigma}_N] \\ \mathcal{O}_5 &= \vec{\sigma}_L \cdot (i\hat{q} \times \vec{v}_N) & \mathcal{O}'_{13} &= \vec{\sigma}_L \cdot (i\hat{q} \times [\vec{v}_N \times \vec{\sigma}_N]) \\ \mathcal{O}_6 &= i\hat{q} \cdot \vec{\sigma}_L i\hat{q} \cdot \vec{\sigma}_N & \mathcal{O}_{14} &= i\hat{q} \cdot \vec{\sigma}_L \vec{v}_N \cdot \vec{\sigma}_N \\ \mathcal{O}_7 &= 1_L \vec{v}_N \cdot \vec{\sigma}_N & \mathcal{O}_{15} &= i\hat{q} \cdot \vec{\sigma}_L i\hat{q} \cdot [\vec{v}_N \times \vec{\sigma}_N] \\ \mathcal{O}_8 &= \vec{\sigma}_L \cdot \vec{v}_N & \mathcal{O}'_{16} &= i\hat{q} \cdot \vec{\sigma}_L i\hat{q} \cdot \vec{v}_N \end{aligned} \quad (5)$$

With the inclusion of isospin to allow for distinct proton and neutron couplings, the ET Lagrangian takes the form

$$\mathcal{L} = \sqrt{2}G_F \sum_{\tau=0,1} \sum_{i=1}^{16} \tilde{c}_i \mathcal{O}_i t^\tau \quad (6)$$

where $t^0 = 1$, $t^1 = \tau^3$. The coefficients \tilde{c}_i are the low-energy constants (LECs) that contain the CLFV physics. The tildes denote that \tilde{c} and \tilde{R} (see below) are dimensionless and normalized to the scale $\sqrt{2}G_F$.

The Nuclear Embedding: The embedding of an NRET in a nucleus can have interesting consequences in exclusive processes, enhancing sensitivity to some operators, reducing through selection rules sensitivity to others. The embedding also alters the interpretation of the LECs: various corrections associated with more complicated currents, operator mixing that arises from the incomplete nuclear Hilbert space, and other many-body effects can shift LEC values. The NRET's complete operator basis can accommodate mixing effects that redistribute strength among the operators. The LECs remain a very useful way to represent the CLFV physics extracted from experiment, including correlating results from different targets, but the extracted LECs require some interpretation [9].

One proceeds by generating one-body charge and current operators from Eq. (6) and performing a standard multipole analysis [19]. While this generates 11 nuclear response functions $W_{\mathcal{O}}^{\tau\tau'}$, five are eliminated by parity and CP constraints on elastic scattering [9, 11]. The $\mu \rightarrow e$ decay rate is

$$\omega = \frac{G_F^2}{\pi} \frac{q_{\text{eff}}^2}{1 + \frac{q}{M_T}} |\phi_{1s}^{Z_{\text{eff}}}|^2 \sum_{\tau=0,1} \sum_{\tau'=0,1}$$

$$\begin{aligned}
& \times \left\{ \left[\tilde{R}_M^{\tau\tau'} W_M^{\tau\tau'} + \tilde{R}_{\Sigma''}^{\tau\tau'} W_{\Sigma''}^{\tau\tau'} + \tilde{R}_{\Sigma'}^{\tau\tau'} W_{\Sigma'}^{\tau\tau'} \right] \right. \\
& + \frac{q_{\text{eff}}^2}{m_N^2} \left[\tilde{R}_{\Phi''}^{\tau\tau'} W_{\Phi''}^{\tau\tau'} + \tilde{R}_{\Phi'}^{\tau\tau'} W_{\Phi'}^{\tau\tau'} + \tilde{R}_{\Delta}^{\tau\tau'} W_{\Delta}^{\tau\tau'} \right] \\
& \left. - \frac{2q_{\text{eff}}}{m_N} \left[\tilde{R}_{\Phi''M}^{\tau\tau'} W_{\Phi''M}^{\tau\tau'} + \tilde{R}_{\Delta\Sigma'}^{\tau\tau'} W_{\Delta\Sigma'}^{\tau\tau'} \right] \right\} \quad (7)
\end{aligned}$$

where M_T is the target mass, and $\phi_{1s}^{Z_{\text{eff}}}$ is a Coulomb factor described below. This result agrees with the general rate formula deduced from symmetry considerations [9] and provides microscopic forms for the nuclear response functions $W_{\mathcal{O}}^{\tau\tau'}(q_{\text{eff}})$, allowing them to be evaluated in the shell model. These response functions can be viewed as ‘‘dials’’ that an experimentalist can tune by selecting appropriate targets.

The operator notation is standard in semi-leptonic weak interactions [11, 26], corresponding to charge M_J , longitudinal spin Σ_J'' , transverse electric spin Σ_J' , and transverse magnetic velocity Δ_J operators. The longitudinal Φ_J'' and transverse electric $\tilde{\Phi}_J'$ operators are generated from the spin-velocity current $\vec{v}_N \times \vec{\sigma}_N$. CP and parity limit the contributing J to even ($M_J, \Phi_J'', \tilde{\Phi}_J'$) or odd ($\Sigma_J'', \Sigma_J', \Delta_J$) values. The multipole operators are defined in [9]. Taking $m_N \rightarrow \infty$ in Eq. (7) yields the point-nucleus rate.

The $\tilde{R}_{\mathcal{O}}^{\tau\tau'}$ are our key result, as they define what can be learned from elastic $\mu \rightarrow e$ conversion:

$$\begin{aligned}
\tilde{R}_M^{\tau\tau'} &= \tilde{c}_1^\tau \tilde{c}_1^{\tau'*} + \tilde{c}_{11}^\tau \tilde{c}_{11}^{\tau'*} \\
\tilde{R}_{\Phi''}^{\tau\tau'} &= \tilde{c}_3^\tau \tilde{c}_3^{\tau'*} + (\tilde{c}_{12}^\tau - \tilde{c}_{15}^\tau) (\tilde{c}_{12}^{\tau'*} - \tilde{c}_{15}^{\tau'*}) \\
\tilde{R}_{\Phi''M}^{\tau\tau'} &= \text{Re} \left[\tilde{c}_3^\tau \tilde{c}_1^{\tau'*} - (\tilde{c}_{12}^\tau - \tilde{c}_{15}^\tau) \tilde{c}_{11}^{\tau'*} \right] \\
\tilde{R}_{\Phi'}^{\tau\tau'} &= \tilde{c}_{12}^\tau \tilde{c}_{12}^{\tau'*} + \tilde{c}_{13}^\tau \tilde{c}_{13}^{\tau'*} \\
\tilde{R}_{\Sigma''}^{\tau\tau'} &= (\tilde{c}_4^\tau - \tilde{c}_6^\tau) (\tilde{c}_4^{\tau'*} - \tilde{c}_6^{\tau'*}) + \tilde{c}_{10}^\tau \tilde{c}_{10}^{\tau'*} \\
\tilde{R}_{\Sigma'}^{\tau\tau'} &= \tilde{c}_4^\tau \tilde{c}_4^{\tau'*} + \tilde{c}_9^\tau \tilde{c}_9^{\tau'*} \\
\tilde{R}_{\Delta}^{\tau\tau'} &= \tilde{c}_5^\tau \tilde{c}_5^{\tau'*} + \tilde{c}_8^\tau \tilde{c}_8^{\tau'*} \\
\tilde{R}_{\Delta\Sigma'}^{\tau\tau'} &= \text{Re} \left[\tilde{c}_5^\tau \tilde{c}_4^{\tau'*} + \tilde{c}_8^\tau \tilde{c}_9^{\tau'*} \right]. \quad (8)
\end{aligned}$$

A program of $\mu \rightarrow e$ conversion experiments can in principle place eight constraints on the LECs. Four CLFV ET operators, $\mathcal{O}_2, \mathcal{O}_7, \mathcal{O}_{14}$, and \mathcal{O}_{16} , are not probed due to parity and CP constraints.

Limits on the LECs can be obtained from experiment, using shell-model calculations of the nuclear response functions. As the CLFV LEC space has 32 degrees of freedom, we turn on each LEC separately to assess sensitivity along each operator ‘‘axis’’ in this space. The LEC limits obtained from the existing Ti branching ratio bound [13] and from a projected ^{27}Al limit of 10^{-17} are shown in Table I. Targets differ in sensitivity to the various operators, re-

TABLE I. LEC limits imposed by the indicated $\mu \rightarrow e$ conversion branching ratios. E- $x \equiv 10^{-x}$.

LEC	Target (Branching Ratio)			
	Al (10^{-17})		Ti (6.1E-13)	
	$\tau = 0$	$\tau = 1$	$\tau = 0$	$\tau = 1$
$ \tilde{c}_1 , \tilde{c}_{11} $	4.0E-10	1.2E-8	7.4E-8	1.3E-6
$ \tilde{c}_3 , \tilde{c}_{15} $	1.6E-8	1.9E-7	3.8E-6	7.3E-6
$ \tilde{c}_4 $	1.4E-8	1.7E-8	1.5E-5	1.7E-5
$ \tilde{c}_5 , \tilde{c}_8 $	7.8E-8	1.2E-7	5.8E-5	6.5E-5
$ \tilde{c}_6 , \tilde{c}_{10} $	2.0E-8	2.2E-8	1.8E-5	2.0E-5
$ \tilde{c}_9 $	2.1E-8	2.8E-8	2.8E-5	3.4E-5
$ \tilde{c}_{12} $	1.6E-8	1.4E-7	3.8E-6	7.3E-6
$ \tilde{c}_{13} $	1.8E-6	2.1E-7	8.4E-5	3.7E-4

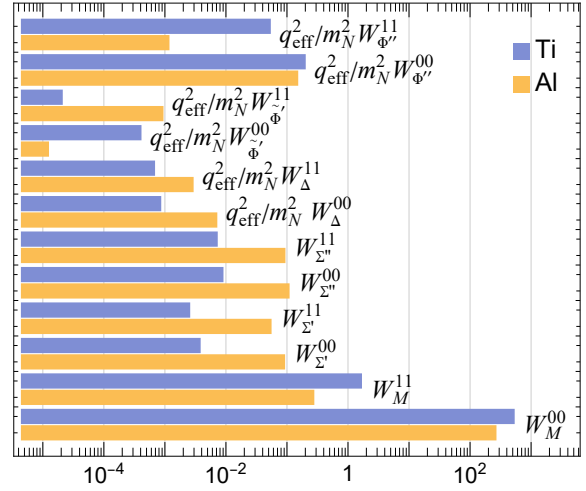


FIG. 2. Comparison of Al and Ti response functions, which govern sensitivities to the CLFV bilinears defined in the text.

flecting aspects of their ground-state structure. We compare the strength of nuclear responses in Al and Ti in Fig. 2. The next-generation target ^{27}Al proves to be versatile in its range of sensitivities [9].

The tabulated LEC limit can be converted into a CLFV mass scale through the relation

$$\Lambda_i^\tau \sim \frac{(\sqrt{2}G_F)^{-1/2}}{\sqrt{|\tilde{c}_i^\tau|}} \sim \frac{246.2 \text{ GeV}}{\sqrt{|\tilde{c}_i^\tau|}} \quad (9)$$

The LECs \tilde{c}_1^0 and \tilde{c}_{11}^0 , for which the nuclear response is fully coherent, will be probed by Mu2e and COMET at scales $\gtrsim 10^4$ TeV, while most of the remaining couplings are tested at levels $\sim 10^3$ TeV.

Nuclear physics, enhancement, selection rules: Nuclear response functions were evaluated using fully correlated shell-model wave functions constructed from Slater determinants in a harmonic oscillator basis. As the calculations are performed in

complete spaces without truncation, we are able to project out spurious center-of-mass motion, preserving Galilean invariance. Wave functions for ^{27}Al and Ti were computed using BIGSTICK [27, 28] and the USDB $2s1d$ [29] and KB3G $2p1f$ [30] interactions, respectively. The Ti calculations were summed over stable isotopes, weighted by their abundance. The adopted oscillator parameters b of 1.84 and 1.99 fm for Al and Ti, respectively, are consistent with the r.m.s. charge radii of these nuclei.

The nuclear embedding alters the NRET: First, the nucleus can enhance interactions due to coherence. It is well known that the isoscalar monopole operator M_0 is coherently enhanced, and thus when it is present it dominates the rate. In our NRET, a second monopole charge operator Φ_0'' is generated from the spin-velocity current $\vec{\sigma}_N \times \vec{v}_N$, which is associated with tensor-mediated interactions such as

$$\bar{\chi}_e i\sigma^{\mu\nu}\gamma^5\chi_\mu \bar{N}i\sigma_{\mu\nu}\gamma^5 N. \quad (10)$$

Enhancement occurs in nuclei where one shell of a spin-orbit pair is filled and the other empty: this is the case for Al (filled $1d_{5/2}$, empty $1d_{3/2}$). Although the pseudotensor interaction above generates a coupling to both nuclear charge and spin—so that \vec{v}_N -dependent contributions might be expected to be a small correction—they in fact double the rate [9].

Second, in elastic $\mu \rightarrow e$ conversion, nuclear selection rules can blind one to certain NRET operators. For example, multipoles of the axial charge $\vec{\sigma}_N \cdot \vec{v}_N$ violate either P or CP and thus cannot contribute to the ground-state nuclear process. Such operators are probed only in inelastic $\mu \rightarrow e$ conversion.

Response functions and \vec{v}_μ : The response functions in Eq. (7) involve the convolution of a multipole nuclear density with a gently varying muon wave function: in Al, the muon's Bohr radius ~ 20 f.

$$W_O \equiv \frac{4\pi}{2j_N + 1} \sum_J |\langle j_N || \hat{O}_J^g(q) || j_N \rangle|^2$$

$$\hat{O}_J^g = \sum_{i=1}^A \frac{1}{\sqrt{4\pi}} g(x_i) \hat{O}_{JM}(qx_i) \quad (11)$$

A common practice, employed in Eq. (7), replaces the muon wave function by an average value,

$$W_O \rightarrow |\phi_{1s}^{Z_{\text{eff}}}|^2 \frac{4\pi}{2j_N + 1} \sum_J |\langle j_N || \hat{O}_J(q) || j_N \rangle|^2$$

$$\hat{O}_J = \sum_{i=1}^A \hat{O}_{JM}(qx_i) \quad (12)$$

The most frequently used procedure for performing this averaging is borrowed from the inclusive process

of muon capture and is not optimal [9]. We define $\phi_{1s}^{Z_{\text{eff}}}$ to reproduce the exact value of the monopole charge amplitude and then use this value for all other response functions. In Al, the average error induced in the rate by this approximation is 1.8% [9], much less than typical nuclear structure errors in evaluating the response functions. While it is not strictly necessary, the use of $\phi_{1s}^{Z_{\text{eff}}}$ greatly simplifies the nuclear physics, permitting all nuclear matrix elements to be expressed as polynomial functions of y .

The NRET can be extended to include all effects linear in \vec{v}_μ [9], yielding a small correction to the nuclear responses

$$W_O \rightarrow \frac{4\pi}{2j_N + 1} \sum_J |\langle j_N || \hat{O}_J^g + \hat{O}_J^f || j_N \rangle|^2 \quad (13)$$

where the new term is defined in analogy with \hat{O}_J^g with $g(r) \rightarrow f(r)$. The form of the rate is unchanged: \vec{v}_μ only alters the nuclear form factors at the level $\sim 2|\langle f \rangle / \langle g \rangle| \sim 5\%$ in ^{27}Al . In the literature, \vec{v}_μ has been included by truncating the multipole expansion at leading order, a procedure that, depending on the operator, can introduce errors that exceed the intended relativistic muon correction [9].

Technical details of the work reported here, a discussion of the related CLFV processes $\mu \rightarrow e\gamma$ and $\mu \rightarrow 3e$, and a description of publicly-available Mathematica and Python scripts that can be used for EFT analysis may be found in [9].

The authors would like to thank Michael J. Ramsey-Musolf for extensive discussions. This work was supported in part by the US Department of Energy under grants DE-SC0004658, DE-SC0015376, and DE-AC02-05CH11231, by the National Science Foundation under cooperative agreements 2020275 and 1630782, and by the Heising-Simons Foundation under award 00F1C7.

-
- [1] S. Davidson, B. Echenard, R. H. Bernstein, J. Heeck and D. G. Hitlin, (arXiv:2209.00142).
 - [2] R. Barbieri and L. J. Hall, Phys. Lett. B **338**, 212-218 (1994).
 - [3] V. Cirigliano, R. Kitano, Y. Okada and P. Tuzon, Phys. Rev. D **80**, 013002 (2009).
 - [4] L. Calibbi and G. Signorelli, Riv. Nuovo Cimento **41**, 71 (2018).
 - [5] L. Bartoszek et al. (The Mu2E Collaboration), Fermilab-TM-2594 and Fermilab-DESIGN-2014-1 (arXiv:1501.05241).
 - [6] F. Abusalma et al., (Fermilab report FN-1052 (arXiv:1802.02599)).
 - [7] R. Abramishvili et al. (The COMET Collaboration), Prog. Theor. Exp. Phys. **2020**, 033C01 (2020).

- [8] J.-C. Angelique et al. (COMET Collaboration), arXiv:1812.07824.
- [9] W. C. Haxton, Evan Rule, Kenneth McElvain, and Michael J. Ramsey-Musolf, arXiv:2208.07945 (submitted to Phys. Rev. C)
- [10] A. L. Fitzpatrick, W. C. Haxton, E. Katz, N. Lubbers, and Y. Xu, JCAP **02**, 004 (2013)
- [11] N. Anand, A. L. Fitzpatrick, and W. C. Haxton, Phys. Rev. C **89**, 065501 (2014).
- [12] M. Baumgart, F. Bishara, J. Brod, T. Cohen, A. L. Fitzpatrick et al., arXiv:2203.08204 (Snowmass whitepaper)
- [13] P. Wintz, Proc. 1st Int. Symp. on Lepton and Baryon Number Violation, ed. by H. V. Klapdor-Kleingrothaus and I. V. Krivosheina (IOP Publishing, Bristol and Philadelphia, 1998), p. 534.
- [14] A. Czarnecki, W. J. Marciano, and K. Melnikov, ASIP Conf. Proc. **435**, 409 (1988).
- [15] R. Kitano, M. Koike, and Y. Okada, Phys. Rev. D **66**, 096002 (2002).
- [16] A. Crivellin, M. Hoferichter, and M. Procura, Phys. Rev. D **89**, 054021 (2014).
- [17] A. Bartolotta and M. J. Ramsey-Musolf, Phys. Rev. C **98**, 015208 (2018).
- [18] V. Cirigliano, K. Fuyuto, M. J. Ramsey-Musolf and E. Rule, Phys. Rev. C **105**, 055504 (2022) doi:10.1103/PhysRevC.105.055504 [arXiv:2203.09547 [hep-ph]].
- [19] J. D. Walecka, in *Muon Physics, Vol II*, ed. V. W. Hughes and C. S. Wu (Academic Press, New York, 1975).
- [20] H. De Vries, C. W. De Jager, and C. De Vries, Atomic Data and Nucl. Data Tables **36**, 495 (1987).
- [21] F. Lenz, Ph.D. thesis, Freiburg, Germany (1971).
- [22] J. Knoll, Nucl. Phys. A **223**, 462 (1974).
- [23] F. Lenz and R. Rosenfelder, Nucl. Phys. A **176**, 513 (1971).
- [24] B. D. Serot, Nucl. Phys. A **308**, 457 (1978).
- [25] T. Suzuki, D. F. Measday, and J. P. Roalsvig, Phys. Rev. C **35**, 2212 (1987).
- [26] T. W. Donnelly and W. C. Haxton, Atomic Data and Nucl. Data Tables **23**, 103 (1979).
- [27] C. W. Johnson, W. E. Ormand, and P. G. Krastev, Comp. Phys. Comm. **184**, 2671 (2013).
- [28] C. W. Johnson, W. E. Ormand, K. S. McElvain, and H. Z. Shan, arXiv:1801.08432 (Report LLNL-SM-739926) (2018).
- [29] B. A. Brown and W. A. Richter, Phys. Rev. C **74**, 034315 (2006).
- [30] A. Poves, J. Sánchez-Solano, E. Caurier, and F. Nowacki, Nucl. Phys. A **694**, 157 (2001).
- [31] T. Mori et al., Nuovo Cim. C **39**, 325 (2017).
- [32] A. M. Baldini et al., Eur. Phys. J. C **78**, 380 (2018).